M13 Bacteriophage as a Biological Scaffold for Magnetically-Recoverable Metal Nanowire Catalysts: Combining Specific and Nonspecific Interactions To Design Multifunctional Nanocomposites

Kendra N. Avery, Janell E. Schaak, and Raymond E. Schaak*

Department of Chemistry and Materials Research Institute, The Pennsylvania State University, University Park, Pennsylvania 16802

Received March 29, 2009
Revised Manuscript Received April 23, 2009

Biological molecules and organisms are intriguing scaffolds for the growth and assembly of inorganic nanoparticles. Biopolymers such as DNA,[1,2] RNA,[3,4] and proteins[5−13] have been used to template the synthesis and spatial organization of metal and semiconductor nanoparticles, and bacteria,[14−16] viruses,[17−20] yeast,[21] and fungi[22] have been used for similar purposes. These biological templates are useful because of their molecularly precise shapes and the spatial organization that they impart on the nanoparticles, as well as specific affinities for binding to surfaces and nucleating and assembling certain materials.[23,24] In particular, the M13 bacteriophage has been used extensively for its ability to bind selectively to a variety of distinct crystal faces of several types of materials.[25] It has also been shown to template the formation of nanocrystals,[26] nucleate the precipitation of crystalline powders,[27,28] and assemble nanocrystals into highly organized nanostructures.[29] M13 bacteriophage that exhibit these material-specific binding and nucleation capabilities are typically identified through a multistep biopanning process.[27,30] These studies generally yield a small number of amino acid sequences that are thought to be responsible for the specific phage/surface interactions. Binding occurs either via the tip of the bacteriophage (pIII region) or, through genetic modification, both the tip and body (pVIII region).[26,31] As a result, nanoparticles can form at the tips or decorate the bacteriophage lengthwise to generate nanowires.[26,31]

Most of the efforts involving materials applications of the M13 bacteriophage have centered on identifying and exploiting binding motifs that are specific for a particular material or crystal face, with genetic engineering of the pVIII region required for nucleating nanoparticles lengthwise to form nanowires. Typically, a single material is templated by the phage, although a few examples of phage-templated nanoparticle composites are known (e.g., Co_3O_4/Au[32] and Au/CdSe[33]). Here, we show that nonspecific electrostatic interactions between cationic aqueous metal complexes and the anionic carboxylate groups of the solvent-exposed pVIII region of wild-type (WT) M13 bacteriophage, followed by borohydride reduction, can generate similar nanostructures without the need for genetic modification. These nonspecific electrostatic interactions can also be used to template metal particles lengthwise along the pVIII region of M13 bacteriophage that have previously been selected for specificity to a different material at the tip (pIII region) via phage display. This approach to site-directed templating via a combination of specific and nonspecific interactions can be

* Corresponding author. E-mail: schaak@chem.psu.edu.

(1) Alivisatos, A. P.; Johnsson, K. P.; Peng, X.; Wilson, T. E.; Loweth, C. J.; Bruchez, M. P., Jr.; Schultz, P. G. *Nature* **1996**, *382*, 609–611.
(2) Storhoff, J. J.; Mirkin, C. A *Chem. Rev.* **1999**, *99*, 1849–1862.
(3) Gugliotti, L. A.; Feldheim, D. L.; Eaton, B. E. *Science* **2004**, *304*, 850–852.
(4) Ma, N.; Dooley, C. J.; Kelley, S. O. *J. Am. Chem. Soc.* **2006**, *128*, 12598–12599.
(5) Slocik, J. M.; Wright, D. W. *Biomacromolecules* **2003**, *4*, 1135–1141.
(6) Kim, J. W.; Choi, S. H; Lillehei, P. T.; Chu, S. H.; King, G. C.; Watt, G. D. *Chem. Commun.* **2005**, 4101–4103.
(7) Banerjee, I. A.; Yu, L.; Matsui, H. *J. Am. Chem. Soc.* **2005**, *127*, 16002–16003.
(8) (a) Slocik, J. M.; Tam, F.; Halas, N. J.; Naik, R. R. *Nano Lett.* **2007**, *7*, 1054–1058. (b) Dickerson, M. B.; Sandhage, K. H.; Naik, R. R. *Chem. Rev.* **2008**, *108*, 4935–4978.
(9) Chen, C. L.; Zhang, P.; Rosi, N. L. *J. Am. Chem. Soc.* **2008**, *130*, 13555–13557.
(10) Brutchey, R. L.; Yoo, E. S.; Morse, D. E. *J. Am. Chem. Soc.* **2006**, *128*, 10288–10294.
(11) Tahir, M. N.; Eberhardt, M.; Therese, H. A.; Kolb, U.; Theato, P.; Muller, W. E. G.; Schroder, H. C.; Tremel, W. *Angew. Chem., Int. Ed.* **2006**, *45*, 4803–4809.
(12) Parker, M. J.; Allen, M. A.; Ramsay, B.; Klem, M. T.; Young, M.; Douglas, T. *Chem. Mater.* **2008**, *20*, 1541–1547.
(13) Goede, K.; Busch, P.; Grundman, M. *Nano Lett.* **2004**, *4*, 2115–2120.
(14) Bharde, A. A.; Parikh, R. Y.; Baidakova, M.; Jouen, S.; Hannyer, B.; Enoki, T.; Prasad, B. L. V.; Shouche, Y. S.; Ogale, S.; Sastry, M. *Langmuir* **2008**, *24*, 5787–5794.
(15) Lengke, M. F.; Fleet, M. E.; Southam, G. *Langmuir* **2006**, *22*, 2780–2787.
(16) He, Y.; Yuan, J.; Su, F.; Xing, X.; Shi, G. *J. Phys. Chem. B* **2006**, *110*, 17813–17818.
(17) Lee, S. W.; Mao, C.; Flynn, C. E.; Belcher, A. M. *Science* **2002**, *296*, 892–895.
(18) Mao, C.; Solis, D. J.; Reiss, B. D.; Kottmann, S. T.; Sweeney, R. Y.; Hayhurst, A.; Georgiou, G.; Iverson, B.; Belcher, A. M. *Science* **2004**, *303*, 213–217.
(19) Tsukamoto, R.; Muraoka, M.; Seki, M.; Tabata, H.; Yamashita, I. *Chem. Mater.* **2007**, *19*, 2389–2391.
(20) Dujardin, E.; Peet, C.; Stubbs, G.; Culver, J. N.; Mann, S. *Nano Lett.* **2003**, *3*, 413–417.
(21) Peele, B. R.; Krauland, E. M.; Wittrup, K. D.; Belcher, A. M. *Langmuir* **2005**, *21*, 6929–6933.
(22) Bansal, V.; Poddar, P.; Ahmad, A.; Sastry, M. *J. Am. Chem. Soc.* **2006**, *128*, 11958–11963.
(23) Sotiropoulou, S.; Sierra-Sastre, Y.; Mark, S. S.; Batt, C. A. *Chem. Mater.* **2008**, *20*, 821–834.
(24) Gazit, E. *FEBS J.* **2006**, *274*, 317–322.
(25) Whaley, S. R.; English, D. S.; Hu, E. L.; Barbara, P. F.; Belcher, A. M. *Nature* **2000**, *405*, 665–668.
(26) Mao, C.; Flynn, C. E.; Hayhurst, A.; Sweeney, R.; Qi, J.; Georgiou, G.; Iverson, B.; Belcher, A. M. *Proc. Natl. Acad. Sci. U.S.A.* **2003**, *100*, 6946–6951.
(27) Ahmad, G.; Dickerson, M. B.; Church, B. C.; Cai, Y.; Jones, S. E.; Naik, R. R.; King, J. S.; Summers, C. J.; Kroger, N.; Sandhage, K. H. *Adv. Mater.* **2007**, *18*, 1759–1763.
(28) Ahmad, G.; Dickerson, M. B.; Cai, Y.; Jones, S. E.; Ernst, E. M.; Haluska, M. S.; Wang, J.; Subramanyam, G.; Naik, R. R.; Kroger, N.; Sandhage, K. H. *J. Am. Chem. Soc.* **2008**, *130*, 4–5.
(29) Nam, K. T.; Peelle, B. R.; Lee, S. W.; Belcher, A. M. *Nano Lett.* **2004**, *4*, 23–27.
(30) Seeman, N. C.; Belcher, A. M. *Proc. Natl. Acad. Sci.* **2002**, *99*, 6451–6455.
(31) Flynn, C. E.; Mao, C.; Hahurst, A.; Williams, J. L.; Georgou, G.; Inverson, B.; Belcher, A. M. *J. Mater. Chem.* **2003**, *13*, 2414–2421.
(32) Nam, K. T.; Kim, D. W.; Yoo, P. J.; Chiang, C. Y.; Meethong, N.; Hammond, P. T.; Chiang, Y. M.; Belcher, A. M. *Science* **2006**, *312*, 885–888.
(33) Huang, Y.; Chiang, C. Y.; Lee, S. K.; Gao, Y.; Hu., E. L.; Yoreo, J. D.; Belcher, A. M. *Nano Lett.* **2005**, *5*, 1429–1434.

10.1021/cm900869u CCC: $40.75
Published on Web 05/07/2009

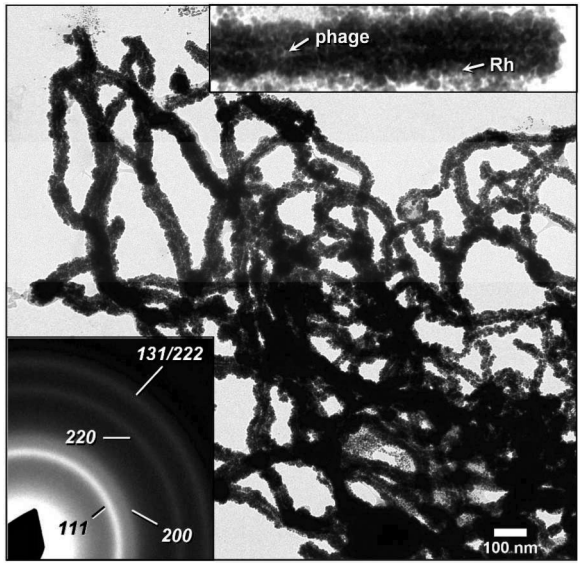

Figure 1. TEM images of WT phage coated with Rh nanoparticles using $RhCl_3$ as the metal salt reagent and SAED pattern confirming the presence of fcc Rh.

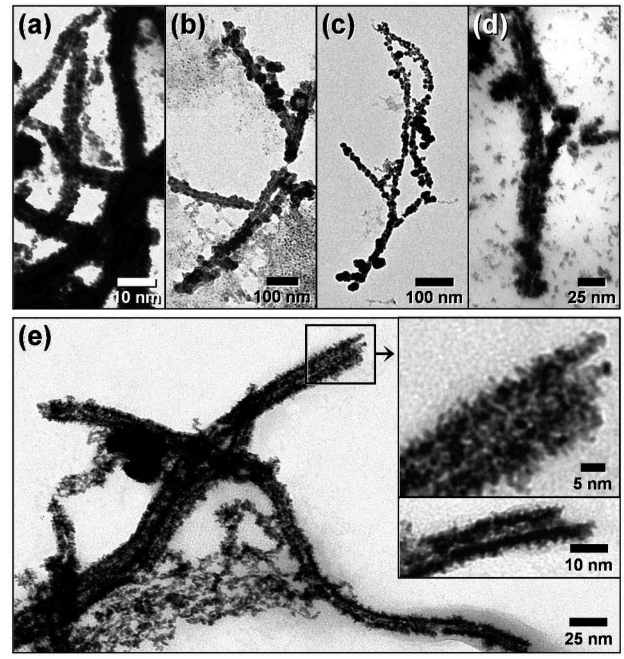

Figure 2. Representative TEM images of WT M13 bacteriophage coated with nanoparticles of (a) Rh (K_3RhCl_6), (b) Ru ($RuCl_3$), (c) Ru (K_3RuCl_6), (d) Pd (K_2PdCl_4), and (e) Pd ($PdCl_2$). Metal salts used for each sample are indicated in parentheses.

used to engineer bifunctional nanocomposite materials. Magnetically separable hydrogenation catalysts (pVIII-Rh/pIII-Fe_3O_4) are used to demonstrate this concept.

Bacteriophage decorated with Rh, Pd, and Ru nanoparticles were typically synthesized by incubating 100 − 200 μL of WT M13 bacteriophage ($\sim 5 \times 10^{12}$ to 2×10^{14} pfu/mL) with 50 μL of 50 mM metal salt solutions ($RhCl_3 \cdot xH_2O$, K_3RhCl_6, $PdCl_2$, K_2PdCl_4, $RuCl_3 \cdot xH_2O$, K_3RuCl_6) in 750 μL of Milli-Q deionized H_2O (autoclaved) at room temperature with gentle mixing for approximately 1 h. The metal salts were reduced by the slow dropwise addition of 50−100 μL of freshly prepared $NaBH_4$ (approximately 25 mg/mL) to the solution of phage and metal salts. The nanoparticle-decorated phage were collected via centrifugation, washed in H_2O and 70% ethanol with brief sonication, and then resuspended in ethanol.

Figure 1 shows transmission electron microscope (TEM) images of Rh nanowires templated by WT M13 bacteriophage. Decorating the phage are aggregates of Rh nanoparticles that are each ~5 nm in diameter. Electron diffraction confirms that the nanoparticles consist of fcc Rh metal (Figure 1). Nanowire formation is likely the result of cationic metal complexes adsorbing nonspecifically along the anionic surface of the pVIII region and remaining anchored after reduction and nucleation of the nanoparticles. This is analogous to the wet impregnation process often used for forming supported metal nanoparticle catalysts[34] and for coating some other types of biological templates.[35] Consistent with this hypothesis, preformed Rh nanoparticles incubated with WT M13 bacteriophage do not assemble into nanowires. Nanowires form only under conditions where a cationic metal reagent is used.

Figure 2 shows representative TEM images for phage-templated Pd and Ru nanowires prepared using a variety of metal salt reagents, including $PdCl_2$, K_2PdCl_4, $RuCl_3 \cdot xH_2O$, and K_3RuCl_6. A different Rh nanowire sample, made using K_3RhCl_6, is also shown (Figure 2a). All of the Rh, Pd, and Ru metal salt reagents exhibit relatively rapid ligand exchange with water, yielding a mixture of predominantly neutral and cationic complexes in near-neutral aqueous solutions, e.g., $Rh(H_2O)_6^{3+}$, $Pd(H_2O)_6^{2+}$, $Ru(H_2O)_6^{3+}$, and other mixed chloro/aqua complexes.[36,37] In contrast, typical Pt and Au metal salts (K_2PtCl_6, $HAuCl_4$) yield predominantly anionic complexes in aqueous solutions near neutral pH.[36,37] Therefore, these anionic species would not be expected to strongly adhere to the negatively charged pVIII surface. Consistent with this, preliminary studies with the Au and Pt systems do not show nanoparticles coating the pVIII surface.

The enlarged TEM images in Figure 2e show that the Pd nanoparticles densely coat the pVIII region of the M13 bacteriophage, but in some cases seem to be absent from the pIII tips. This implies that the pIII region may still be accessible for biopanning and materials-specific binding, and initial studies with the Rh/Fe_3O_4 system support this hypothesis. Six rounds of biopanning were performed against Fe_3O_4 nanoparticles using a commercial library containing $\sim 1 \times 10^9$ random sequences of the 12-mer peptide at the pIII region of the M13 bacteriophage. After the biopanning process was complete, sequencing studies identified the 12-mer QAFPLSNQSLTV as one of several peptides with specificity to our specific sample of Fe_3O_4. This phage (called $\phi_{Fe_3O_4}$) was amplified, and 50 μL of high titer $\phi_{Fe_3O_4}$ was incubated at room temperature overnight with a dispersion

(34) Geus, J. In *Catalyst Preparation: Science and Engineering*; Regalbuto, J.; Ed. Taylor and Frances: Boca Raton, FL, 2007; p 341.
(35) Kumara, M. T.; Muralidharan, S.; Tripp, B. C. *J. Nanosci. Nanotechnol.* **2007**, *7*, 2260–2272.
(36) Cotton, F. A.; Wilkinson, G. *Advanced Inorganic Chemistry*, 5th ed.; Wiley: New York, 1988.
(37) Greenwood, N. N.; Earnshaw, A. *Chemistry of the Elements*, 2nd ed.; Butterworth-Heinemann: Oxford, U.K., 1997.

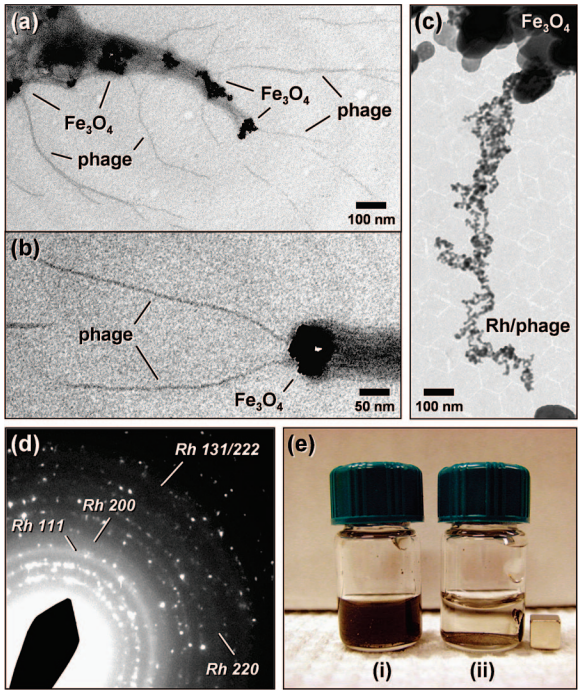

Figure 3. (a, b) Negative-stain TEM images of the $\phi_{Fe_3O_4}$ phage attached to Fe_3O_4 particles via materials-specific interactions after incubating the phage with the particles. (c) TEM image of $\phi_{Fe_3O_4}$ phage coated with Rh nanoparticles and attached to Fe_3O_4 particles. (d) SAED pattern of the Rh/Fe_3O_4/phage sample confirming the presence of Rh (diffuse rings, indexed) and Fe_3O_4 (crystalline spots, see the Supporting Information for comparison). (e) Photograph of aqueous solutions of (i) a uniform dispersion of Rh/Fe_3O_4/phage and (ii) the Rh/Fe_3O_4/phage collected at the side of the vial via interaction with an external magnet.

of Fe_3O_4 nanoparticles. Images a and b in Figure 3 show a negative-stain (2% uranyl acetate) TEM image of $\phi_{Fe_3O_4}$ bound to the larger Fe_3O_4 nanoparticles.

The $\phi_{Fe_3O_4}$ has the same anionic pVIII region as the WT phage, but the pIII region has been selected to be materials-specific toward Fe_3O_4. To combine the materials-specific interactions of the pIII region with the nonspecific electrostatic interactions possible via the anionic pVIII region, we incubated $\phi_{Fe_3O_4}$ in dilute aqueous $RhCl_3$ solution and reduced with $NaBH_4$ as described earlier. The Rh-coated $\phi_{Fe_3O_4}$, made using a lower concentration of $RhCl_3$ relative to that shown in Figure 1 in an attempt to avoid overgrowth at the pIII tip, was collected by centrifugation, rinsed with water, and then incubated with a dispersion of Fe_3O_4 nanoparticles. The TEM image of the product (Figure 3c) confirms the successful incorporation of both Fe_3O_4 and Rh onto the pIII and pVIII regions of $\phi_{Fe_3O_4}$, respectively. The SAED pattern in Figure 3d further confirms the presence of both Rh and Fe_3O_4. The pVIII region was coated lengthwise with Rh nanoparticles via nonspecific electrostatic interactions while the pIII tip was bound to Fe_3O_4 particles via materials-specific interactions. When a magnet is placed next to the vial containing the dispersed Rh/Fe_3O_4 phage, the entire black-colored sample collects at the magnet and leaves behind a clear, colorless solution (Figure 3e). This further confirms that all of the Rh and Fe_3O_4 are co-located on the $\phi_{Fe_3O_4}$, because the Rh are attached to the phage and only the Fe_3O_4 is magnetic.

The M13 bacteriophage provide a high surface area support for nucleating small noble metal nanoparticles with no deliberately added organic stabilizers, making them intriguing for catalytic applications. In particular, Rh nanoparticles are known to be excellent hydrogenation catalysts.[38] As an initial test of their catalytic viability, the hydrogenation of styrene to ethylbenzene was studied. Rh-coated phage (3 mg) was added to 5 mL of a 20 mM solution of styrene in methanol, and the reaction mixture was stirred at room temperature under a hydrogen atmosphere. GC-MS data (see Figure S2 in the Supporting Information) confirmed a complete conversion of styrene to ethylbenzene after 1 h. The catalytic hydrogenation of methyl red[39] was also studied. Rh-coated phage (2 mg) was added to 5 mL of 46 μM methyl red solution, and the reaction mixture was stirred under a hydrogen atmosphere for 10 min. UV−vis spectra (see Figure S3 in the Supporting Information) show a rapid decrease in absorbance of the methyl red solution, indicating the near complete cleavage of the azo bond.[39] The Pd/WT-phage system behaved similarly. These results demonstrating catalytic viability, coupled with the magnetic separation of Rh/Fe_3O_4/phage, provide evidence that specific and nonspecific interactions can be combined for the nucleation and assembly of bifunctional nanocomposites.

In conclusion, nonspecific electrostatic interactions between cationic metal complexes and the anionic pVIII region of WT M13 bacteriophage can be used to generate metal nanowires. These nonspecific interactions along the pVIII region can be combined with materials-specific interactions in the pIII region to engineer multifunctional nanocomposites, such as magnetically separable Rh/Fe_3O_4/phage hydrogenation catalysts. This provides a straightforward platform for designing site-directed multifunctionality into commercially available M13 bacteriophage and serves as a simple method for introducing multicomponent architectures into phage-based scaffolds without the need for genetic engineering.

Acknowledgment. This work was supported by a Beckman Young Investigator Award, a DuPont Young Professor Grant, a Sloan Research Fellowship, a Camille Dreyfus Teacher-Scholar Award, the Petroleum Research Fund (administered by the American Chemical Society), and the U.S. Department of Energy (DE-FG02-08ER46483). The authors thank Dr. Ryland Young for the WT M13 bacteriophage. TEM was performed in the Electron Microscopy Facility, DNA sequencing was performed at the Nucleic Acid Facility, and GC-MS was performed at the Proteomics and Mass Spectrometry Core Facility, all part of the Huck Institutes of the Life Sciences.

Supporting Information Available: Experimental details, bacteriophage cartoon, and additional diffraction, TEM, and catalysis data (PDF). This material is available free of charge via the Internet at http://pubs.acs.org.

CM900869U

(38) Roucoux, A.; Nowicki, A.; Philippot, K. *Nanoparticles and Catalysis*; Astruc, D., Ed.; Wiley: New York, 2008; Chapter 11.
(39) Formo, E.; Lee, E.; Campbell, D.; Xia, Y. *Nano Lett.* **2008**, *8*, 668–672.